Annals of Nuclear Medicine Vol. 7, No. 1, 29–38, 1993

Dopamine D_2 receptor SPECT imaging: Basic *in vivo* characteristics and clinical applications of ^{123}I-IBZM in humans

Hiroshi TOYAMA,*† Masanori ICHISE,* James R. BALLINGER,*
Luis FORNAZZARI** and Joel C. KIRSH*

*Division of Nuclear Medicine, Department of Radiological Sciences, Mount Sinai Hospital
**Clarke Institute of Psychiatry, University of Toronto, Toronto, Canada
†Present address: Department of Radiology, Fujita Health University, Toyoake, Japan

The purposes of this study are to evaluate the utility of kit formulation, the basic *in vivo* characteristics, and clinical usefulness of dopamine D_2 receptor imaging with ^{123}I-(S)-(–)-3-iodo-2-hydroxy-6-methoxy-N-[(1-ethyl-2-pyrrodinyl)methyl]-benzamide (^{123}I-IBZM). We studied 22 normal controls, 3 early symptomatic Huntington's disease patients, and 1 patient with visual hallucination on and off neuroleptics. ^{123}I-IBZM could be conveniently prepared with a high degree of purity from a kit, but with relatively low radiochemical yield. We demonstrated ^{123}I-IBZM receptor binding equilibrium by performing serial SPECT scanning in a normal volunteer. The basal ganglia/frontal cortex (BG/FC) ratios plateaued after the specific binding reached equilibrium approximately 60 minutes after injection. The BG/FC ratio declined significantly with age. The ratios for the Huntington's disease patients were significantly lower than those for normal controls. The images of the patient off neuroleptic therapy showed dramatically increased BG activity compared with those obtained while on therapy. The BG/FC ratio provides an estimate of B_{max}/K_d and hence the receptor density. It appears important to perform SPECT early in the equilibrium phase and at a fixed time after injection to obtain significantly high signal to noise ratios. ^{123}I-IBZM is an ideal tracer for SPECT including a rotating gamma camera type which can provide estimates of the receptor density objectively by calculating the BG/FC ratio, and is a promising agent for the investigation of dopamine D_2 receptors in clinical conditions.

Key words: single photon emission computed tomography (SPECT), ^{123}I-(S)-(–)-3-iodo-2-hydroxy-6-methoxy-N-[(1-ethyl-2-pyrrodinyl)methyl]-benzamide (^{123}I-IBZM), dopamine D_2 receptor, Huntington's disease, equilibrium analysis

INTRODUCTION

RECENTLY, SEVERAL KINDS of neuroreceptor imaging tracers for single photon emission computed tomography (SPECT) have been designed.[1] A major advantage of functional brain imaging over post-mortem studies is that it provides insight into receptor changes at various stages of illness as well as follow-up data on and pharmacological modification of such changes.[2] Although the resolution and sensitivity of positron emission tomography (PET) are superior to those of SPECT,[3] SPECT is much more widely available.

There has been much clinical and pharmacological interest in the use of dopamine D_2 agonists to treat Parkinson's disease and dopamine D_2 antagonists as antipsychotic drugs. Reflecting this, several basic *in vitro* and *in vivo* imaging studies of dopamine D_2 receptors employing neuroleptic ligands have been recently reported.[4–12] ^{123}I-IBZM is a specific dopa-

A part of this paper was presented at Neuroimaging in Psychiatry: An International Symposium held in London, U.K., February 3–4, 1992 and the 39th Annual Meeting of the Society of Nuclear Medicine held in Los Angeles, CA, USA, June 9–12, 1992.

Received April 3, 1992, revision accepted July 6, 1992.

For reprints contact: Masanori Ichise, M.D., Division of Nuclear Medicine, Department of Radiological Sciences, Mount Sinai Hospital, 600 University Avenue, Toronto, Ontario, CANADA, M5G 1X5.

mine D_2 receptor antagonist with high affinity.[4,5] Using ^{123}I-IBZM, studies of neuropsychiatric diseases such as Huntington's disease,[8,13] Parkinson's disease,[8,14] as well as patients on and off neuroleptic therapy[7,8] have shown the potential for clinical usefulness. We had an opportunity to use a kit formulation for preparation of ^{123}I-IBZM developed recently by Kung et al.[15] from the University of Pennsylvania.

The purposes of this study are to 1) assess the utility of this ^{123}I-IBZM kit as a clinical method, 2) study the basic *in vivo* characteristics in order to determine optimal imaging parameters and establish a normal range, and 3) evaluate its potential clinical usefulness.

MATERIALS AND METHODS

1) Synthesis of ^{123}I-IBZM

^{123}I-IBZM was synthesized by a kit procedure, which involves direct labeling of the non-iodinated precursor, BZM.

A 10 μL aliquot of BZM solution in ethanol (0.4 mg/mL), equivalent to 4 μg BZM, was mixed with 100 μL of 0.5 M ammonium acetate, pH 4.0, and added to a reaction tube containing 10–60 mCi (370–2,220 MBq) sodium ^{123}I-iodide in 40–100 μL dilute sodium hydroxide. The reaction was started by the addition of 10 μL freshly diluted 1.5% peracetic acid. After 10 minutes at room temperature, the reaction was quenched by the addition of 100 μL sodium metabisulfite (300 mg/mL) and the mixture was neutralized by the careful addition of 700 μL sodium bicarbonate (100 mg/mL). The product was taken up on a C-18 extraction cartridge (which had been activated with absolute ethanol followed by sterile distilled water), washed with 5 mL sterile distilled water, and eluted with 1–2.5 mL absolute ethanol. To make the product suitable for injection into patients, the ethanol solution was diluted with 9–18 mL saline (i.e. final ethanol concentration 10–15% v/v) and sterilized by passage through a 0.22-μM membrane filter. Radiochemical purity was determined by chromatography using 8 mm $\times$ 70 mm strips cut from solvent saturation pads (Gelman Sciences Inc.) and developed in ethyl acetate; hydrophilic impurities remained near the origin while ^{123}I-IBZM migrated near the solvent front.

2) Imaging protocols and data analyses

We studied 22 normal control subjects (15 males, 7 females, age range: 20–76, mean $=39.7\pm14.7$ yr), 3 early symptomatic Huntington's disease patients with no significant caudate atrophy as determined by X-ray CT (2 males, 1 female, 51.0 ± 10.4 yr), and one 22-year-old male patient with visual hallucination secondary to alcohol abuse twice, on and off neuroleptics. All Huntington's disease patients took no medication for at least 4 weeks before this study. The patient with visual hallucination had no history of neuroleptic medication before his admission.

After informed consent was obtained, a dose of 5 mCi (185 MBq) of ^{123}I-IBZM was injected intravenously into each subject. In order to reduce the radiation dose to the thyroid gland, potassium iodide (Lugol's solution) was given prior to and for 3 days after the study. Immediately after injection, 1 minute/frame lateral dynamic planar images of the head were acquired for 60 minutes. For brain wash-out analyses, square regions of interest (ROI) ($1.8\times$ 1.8 cm) were placed over the basal ganglia, frontal cortex and cerebellum respectively. SPECT was then carried out for 40 minutes. In one normal volunteer, beginning immediately after injection, 6 serial SPECT scans were obtained, each with a 30 minute acquisition.

SPECT imaging was performed with a truncated single head rotating gamma camera interfaced to a dedicated computer (Elscint 409 ECT). Sixty 36 second images were obtained through a 360° circular rotation with a low energy, medium resolution and sensitivity collimator. The full width at half maximum of the system was 15 mm at clinically relevant count levels. The radius of rotation was 14 cm or less with the subject's head securely positioned in an adjustable head holder. The data were acquired onto a 64×64 matrix. One pixel-thick (approximately 4 mm) transaxial slices were reconstructed with a modified Hanning back projection filter parallel to the canthomeatal (CM) line as determined from a lateral scout image with radioactive markers identifying the external auditory meatus and the outer canthus of the eye. The first order Chang method of attenuation correction (0.12 cm^{-1}) was employed. These transaxial images were then compressed into nine slices. One slice was chosen from these in which the basal ganglia were best visualized, and another in which the cerebellum was seen. ROI were drawn manually in both right and left basal ganglia (BG), frontal cortex (FC) bilaterally, and both cerebellar hemispheres (CE). These ROIs were approximately 6 cm^3 for each BG, 22 cm^3 for FC, and 30 cm^3 for CE in volume, respectively. Mean counts per pixel were calculated in these regions. For semi-quantitative evaluation, mean basal ganglia/frontal cortex count ratios and mean basal ganglia/cerebellum count ratios were calculated.

RESULTS

1) Radiopharmaceutical Preparation

In ten preparations, the radiochemical yield was $50\pm6\%$ (range 39 to 57%) and the radiochemical

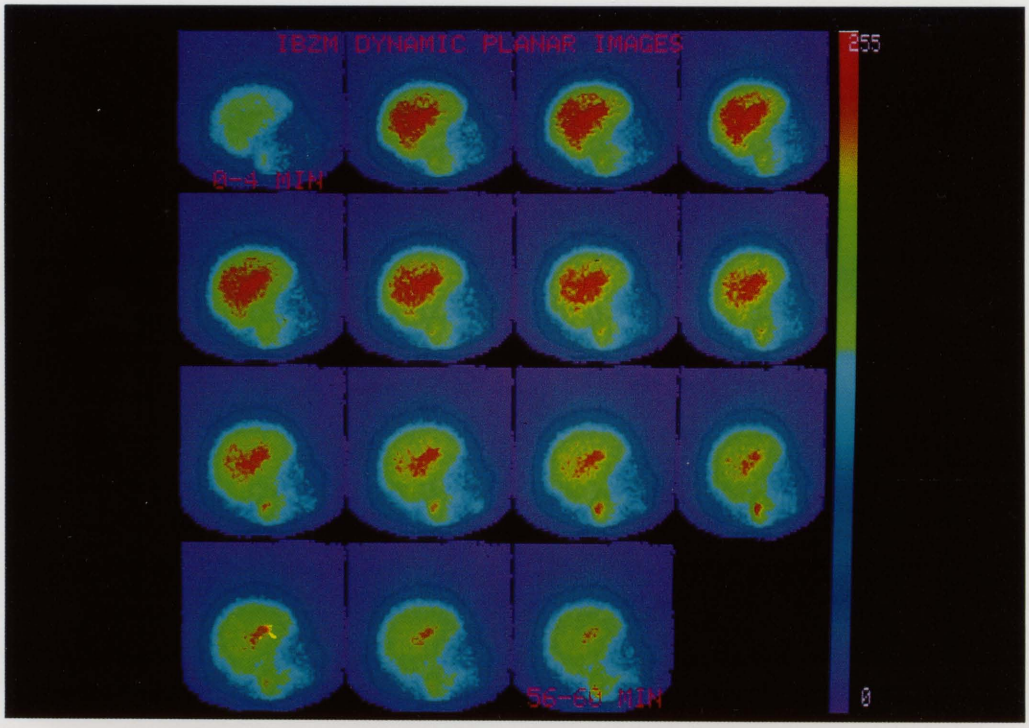

Fig. 1 Summed dynamic lateral planar images of a normal volunteer at 0–4 to 56–60 min post injection. The early phase shows high uptake in the whole brain as well as basal ganglia region. In the later phase, the activity in the basal ganglia region is relatively higher than the other regions.

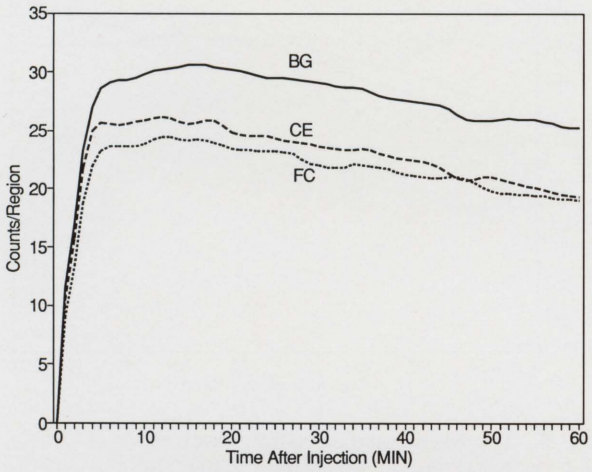

Fig. 2 The 60 minute time activity curve of the dynamic lateral planar scans generated by placing regions of interest on basal ganglia (BG), frontal cortex (FC), and cerebellum (CE) of a normal volunteer. Immediately after injection, all regions showed high uptake followed by gradual wash-out. The basal ganglia activity reached a maximum about 15 minutes post injection.

purity was 94±3% (range 90 to 98%). Total preparation time, including quality control, was approximately 1 hour. Retrospective sterility testing was negative.

2) Imaging and Kinetic study in the brain

Figure 1 shows a set of summed lateral dynamic planar images, and Fig. 2 shows 60 minute time activity curves for the basal ganglia, frontal cortex, and cerebellum of a normal volunteer. In the phase soon after injection, the accumulation of ^{123}I-IBZM was seen in the whole brain as well as in basal ganglia. This brain uptake washed out gradually thereafter. However, the basal ganglia uptake remained relatively higher than uptake in the other regions. The basal ganglia activity reached its maximum about 15 minutes post injection.

In another normal volunteer, beginning immediately after injection, six serial SPECT scans were obtained, each with a 30 minute acquisition. Figure 3 shows a set of 6 serial SPECT images, and Fig. 4 shows 180 minute time activity curves after decay correction for the basal ganglia, frontal cortex, and cerebellum. The wash-out from the cerebellum appeared slightly more marked than that from the frontal cortex. The specific binding of ^{123}I-IBZM in the basal ganglia was calculated as the

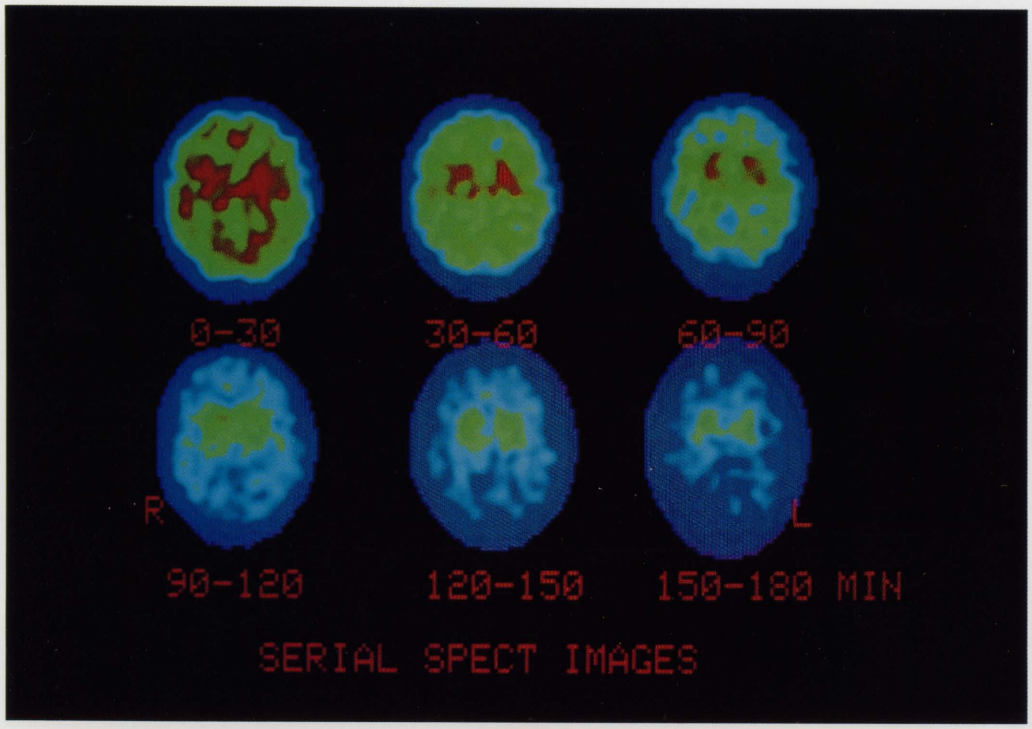

Fig. 3 Six serial SPECT scans of a normal volunteer each with a 30 minute acquisition.

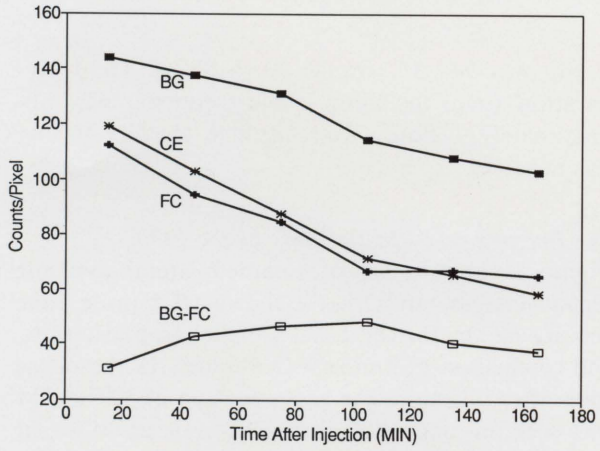

Fig. 4 The 180 minute time activity curves of the 6 serial SPECT scans, for the basal ganglia (BG), frontal cortex (FC), and cerebellum (CE). The specific binding of ^{123}I-IBZM in the basal ganglia was calculated as the difference between basal ganglia and frontal cortex (BG–FC). An equilibrium was seen from 60 to 120 minutes showing binding reversibility.

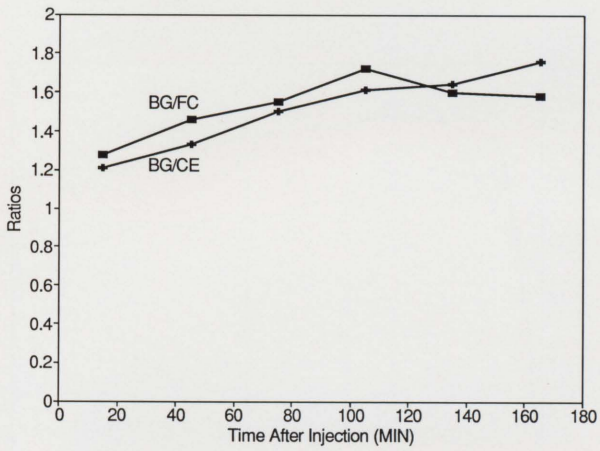

Fig. 5 The basal ganglia/frontal cortex ratios (BG/FC), and the basal ganglia/cerebellum ratios (BG/CE) of the 6 serial SPECT scans. The BG/FC ratios showed an increase until 100 minutes, and then plateaued as the specific binding reached equilibrium. However, the BG/CE ratios showed an increase until 180 minutes.

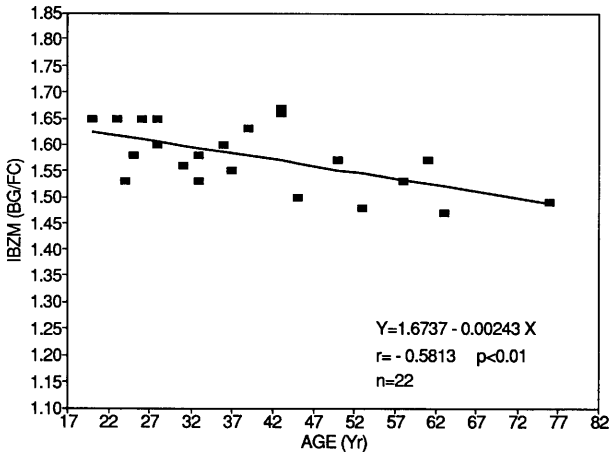

Fig. 6 The age dependency of the basal ganglia/frontal cortex (BG/FC) ratios in normal volunteers. A significant negative correlation was seen with increasing age.

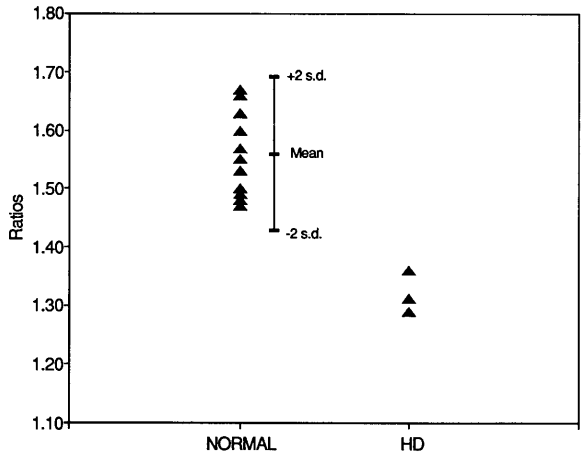

Fig. 7 Comparison of the basal ganglia/frontal cortex (BG/FC) ratios between the age matched normal controls (Normal) (mean=49.4±11.8 yr) and the Huntington's disease patients (HD) (mean=51.0±10.4 yr). The ratios for HD were more than 2 standard deviations below the mean of Normal.

difference between the basal ganglia and frontal cortex. Equilibrium was seen from 60 to 120 minutes, indicating the binding reversibility of ^{123}I-IBZM. Basal ganglia/frontal cortex ratios increased until 100 minutes, and then plateaued as the specific binding reached equilibrium (Fig. 5). In contrast, basal ganglia/cerebellum ratios increased until 180 minutes.

According to the theoretical saturation analysis model[16–18], the basal ganglia/frontal cortex ratio or (Bound+Free)/Free ratio appears to best provide a semiquantitative index for B_{max}/K_d when measurements are made under conditions near equilibrium (See APPENDIX).

3) Normal control value

Two-five million counts/study were obtained. The mean basal ganglia/frontal cortex ratio for 22 normal controls was 1.58±0.06 (range: 1.47–1.67).

4) Effect of age

There was an age dependency of ^{123}I-IBZM uptake in the the basal ganglia. The basal ganglia/frontal cortex ratio declined significantly with increasing age ($r=-0.58$, $p<0.01$) (Fig. 6).

5) Clinical applications

a) Huntington's disease

The basal ganglia/frontal cortex ratios of Huntington's disease patients (mean=51.0±10.4 yr) were significantly lower than those of the 11 age matched normal controls (mean=49.4±11.8 yr) (Fig. 7, Fig. 8).

b) Patient on and off neuroleptics

The patient with visual hallucination secondary to alcohol abuse on an amount of loxapine equivalent to 600 mg/day of chlorpromazine for 2 weeks showed decreased basal ganglia activity, but the uptake dramatically recovered when the patient had been off therapy for 4 weeks prior to re-imaging (Fig. 9).

DISCUSSION

Dopamine receptors are classified into D_1 and D_2 types according to their pharmacological and biochemical characteristics.[19] Stimulation of dopamine D_1 receptors increases adenylate cyclase while D_2 receptor stimulation reduces it. Recently, following cloning of cDNA, two subtypes of dopamine D_2 receptor (D_{2A} and D_{2B}[20–23]), D_3,[24], D_4,[25] and D_5[26] receptors have been identified. The dopamine receptor is localized on pre- and postsynaptic nerve terminals. The presynaptic receptor is also called an autoreceptor, which has characteristics similar to those of a D_2 receptor.[27] The functional role of the D_2 receptor is related to such behavior such as stereotypy, locomotion, vomiting, psychotic activity and normalization of motor activities.[27] Because the D_2 receptor density correlates with the pathophysiology and treatment status of movement disorders such as Parkinson's disease, and psychiatric disorder such as schizophrenia, the characterization of the D_2 receptors has been the first step in basic and clinical investigations.[20,23,27]

Wagner et al. reported for the first time the dopamine receptor imaging using ^{11}C-labeled 3-N-methylspiperone by PET,[28] and Crawley et al. showed SPECT images with ^{77}Br-p-bromo-spiperone.[29] Since spiperone and its derivatives have relatively low specificity (and also bind to serotonin receptors) and

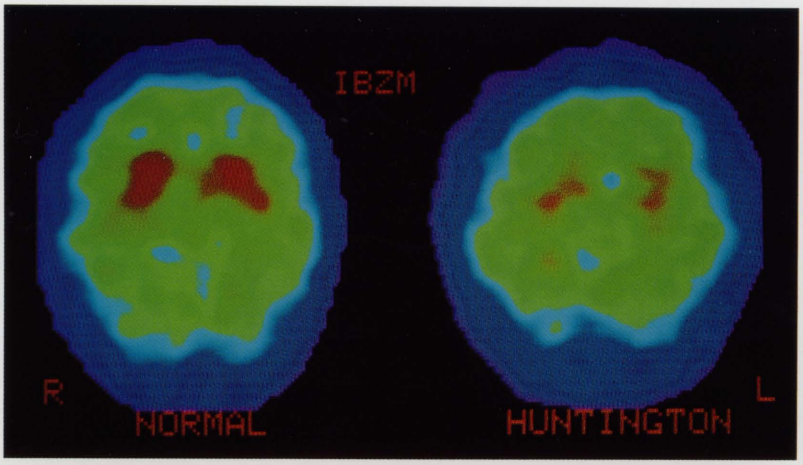

Fig. 8 ^{123}I-IBZM SPECT of a normal volunteer and a Huntington's disease patient. The SPECT of Huntington's disease patient shows markedly decreased basal ganglia uptake bilaterally.

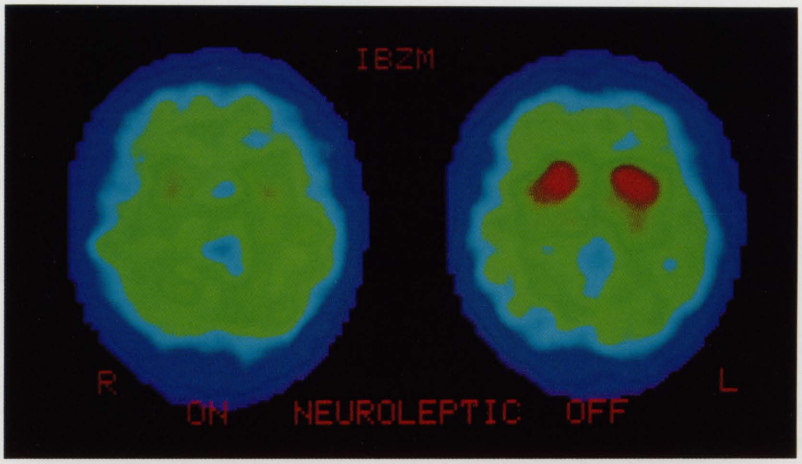

Fig. 9 SPECT of a 22 year old male patient with visual hallucination secondary to alcohol abuse on and off neuroleptic therapy. The first scan while the patient is on neuroleptic therapy for 2 weeks shows markedly reduced basal ganglia uptakes bilaterally {basal ganglia/frontal cortex (BG/FC) ratio: 1.30}. The second scan of the same patient 3 weeks after withdrawal from neuroleptics shows marked recovery in the basal ganglia uptakes (BG/FC ratio: 1.61).

are slow to reach equilibrium, benzamide derivatives have been designed.[16,28] ^{11}C-raclopride, which is one of the derivatives of benzamide, has a high specificity and affinity, and dissociates rapidly from the receptors, allowing binding equilibrium to be established *in vivo* within the time span of a PET experiment.[16,17]

^{123}I-IBZM is also a benzamide derivative, and a close analog of raclopride. *In vivo* binding studies with ^{123}I-IBZM showed both high specificity and high affinity for dopamine D_2 receptors.[4,5] An *in vivo* normal volunteer study with ^{123}I-IBZM showed high uptake in the brain (3.72%), a low radiation dose, and pharmacological safety.[6]

^{123}I-IBZM can be conveniently prepared with a kit procedure which does not require special equipment.[15] The non-iodinated precursor BZM is labeled with ^{123}I by peracetic acid oxidation, then the lipophilic products are separated on an extraction cartridge. This purification does not separate ^{123}I-IBZM from the residual precursor BZM; but the quantity of BZM is small, its binding affinity is much lower than IBZM, and the resultant effective specific activity (–500 Ci/mmol) is suitable for use in patients. The main disadvantage of the kit procedure is its relatively low radiochemical yield (–50%) which makes inefficient use of expensive ^{123}I.

According to our kinetic analyses with 6 serial

SPECT scans over 180 minutes, the specific binding in the basal ganglia reached equilibrium, and washed out thereafter. These findings are consistent with the characteristics of benzamide derivatives which dissociate rapidly from the receptors.[8,9,16,17] There was a tendency towards higher wash-out from the cerebellum than the frontal cortex. For reference regions to evaluate free and nonspecific binding, cerebellum in PET with ^{11}C-raclopride,[16] and frontal cortex in SPECT with ^{123}I-IBZM[7-9] have been chosen. Seeman et al. pointed out that the baseline amount of nonspecific binding of radioactive raclopride to the human striatum is considerably higher than that to the cerebellum from the same human brain.[30] For this reason, Brücke et al. reported that the cerebellum might not be an ideal region for reference, because its nonspecific binding might be lower than that in the striatum.[8] Our preliminary data from one subject could suggest their hypothesis. Dynamic SPECT analyses of several subjects might be helpful in this regard.

The equilibrium basal ganglia/frontal cortex ratio provides an estimate of B_{max}/K_d (Eq. A7) and hence the receptor density, provided that K_d is constant (Eq. A8). Measurements of affinity (K_d) are relatively constant in the rat,[31,32] and no appreciable changes in K_d in postmortem humans whether with age or diseased states such as Parkinson's disease, have been reported.[33-35] Therefore, reductions in the basal ganglia/frontal cortex ratio will reflect the decline in receptor density (B_{max}). This may be due either to degenerative loss of receptors or as a result of D_2 receptor down-regulation. Similarly, rises in the basal ganglia/frontal cortex ratio will reflect the increase in B_{max} as a result of D_2 receptor upregulation secondary to deafferentation.[36] According to the equation (Eq.A7), the basal ganglia/frontal cortex ratio will become constant after equilibrium has been reached. This is in keeping with our results where the ratio plateaued after specific binding equilibrium was reached. A similar result has been reported with ^{11}C-raclopride PET,[36] but conflicting results have also been reported with ^{123}I-IBZM SPECT.[7,9] Although theoretically this ratio should remain constant under conditions after equilibrium, actual regional counts wash out with time. Therefore, measurements made in the later phase may be more subject to statistical error because of the decreased signal to noise ratio. It is, therefore, important to perform SPECT imaging early in the equilibrium phase to obtain sufficient counts. In addition, although imaging at a fixed time after injection may not be required for equilibrium analysis, it may reduce statistical error in comparisons among subjects. Based on our serial SPECT data for one subject and previously reported papers,[8,9] the ideal data collection time is estimated to be between 60 and 120 minutes. The dopamine receptor density can be evaluated objectively with the ratio based on the data of a single SPECT scan of the rotating gamma camera type. Once the imaging timing has been established, serial or continuous dynamic SPECT imaging is no longer required. In terms of a mean basal ganglia/frontal cortex ratio in normal controls, there are slight differences between our data (1.58 ± 0.06) and those of other investigators {1.74 ± 0.11,[8] 1.55 ± 0.05[14]}. This may be due to the differences in the SPECT acquisition timing, choice of reconstruction filter, attenuation correction method, size of ROI used, and SPECT system resolution.[14] Kung et al. reported that one major difference between the no-carrier-added preparation and the kit formulation method is the presence of a small amount of uniodinated BZM in the latter preparation. Because the difference between IBZM and BZM in binding affinity for D_2 receptors is high, the small amount of uniodinated BZM together with the radioactive IBZM will not affect the binding or imaging studies of the labeled IBZM.[12] Actually, regional brain ratios in rats were similar values to the no-carrier-added preparation and the kit formulation method.[12] The basal ganglia/cerebellum ratio of *in vitro* experiments of a monkey was 4.93,[4] and the ratio of *in vitro* autoradiography of mice was 7.3.[5] The main reason for this underestimation of this ratio by means of the SPECT technique is likely to be related to a partial volume effect.[1] In order to reduce statistical sampling error, the smallest volume of ROI in the present study was approximately 6 cm^3 which is roughly $2 \times (\text{FWHM})^3$ of the system used. As the value for Kd increases, the ratio is expected to decrease. However, with PET and ^{11}C-raclopride with a larger value for Kd than that for IBZM, the mean basal ganglia/cerebellum ratio for the normal control was found to be 3.7,[36] which is considerably higher than that for ^{123}I-IBZM SPECT. This can also be explained in terms of the better spatial resolution of the PET system.

It has been observed that endogenous dopamine lowers the apparent density of D_2 receptors detected by the derivatives of benzamide {raclopride,[30,37,38] IBZM[39]}. Seeman et al. reported that the basis for this non competitive behavior between dopamine and raclopride may be related to dopamine's high affinity for the high-affinity state of D_2 receptors. It might be necessary to consider the effect of endogenous dopamine upon the D_2 receptor density measurements with ^{123}I-IBZM. Premedication with reserpine to reduce endogenous dopamine might be useful.[30,39] On the other hand, *in vivo* imaging of D_2 receptor with benzamide derivatives might be useful in estimating the synaptic levels of endogenous

dopamine.[39] Further studies appear to be needed.

The basal ganglia/frontal cortex ratio in this study showed an age dependency as shown by PET[2,40,41] as well as SPECT.[8] *In vitro* animal studies also showed a decrease in dopamine receptors with aging.[31,42] Although decreased dopamine D_2 receptor binding with age in the caudate nucleus has been shown, no such age changes were detected in the putamen in postmortem studies.[33,34] Unfortunately it appears difficult to distinguish the caudate nucleus from putamen accurately by means of SPECT, or even PET.[3] It is suggested that age reduces the functional reserve and adaptive capacity of dopaminergic mechanisms in the basal ganglia.[33] Age matched control subjects must be chosen for comparison with each patient by means of the same equipment.[1,2,40]

The receptor density in early symptomatic Huntington's disease patients showed a significant decrease, presumably because of degenerative loss of postsynaptic D_2 receptors. Our data are consistent with those obtained in PET[43] and SPECT[8] studies. The dopamine D_2 receptor imaging might be promising for early and preclinical detection of Huntington's disease.[13]

The SPECT images of the patient with visual hallucination secondary to alcohol abuse on neuroleptic therapy were significantly different from those obtained when off therapy. These findings show the importance of the timing of imaging to evaluate the receptor status accurately after withdrawal from neuroleptic therapy.[1,7,8]

APPENDIX

From the hyperbolic function equation (16–18),

$$\text{Bound} = \frac{B_{max} \times \text{free}}{K_d + \text{free}} \qquad \text{(Eq. A1)}$$

where B_{max} is the maximal number of receptor sites that specifically bind the ligand, K_d {equilibrium dissociation constant; the dissociation rate constant (k_{off})/the association rate constant (k_{on})} is the ligand concentration at which ligand binding to 50% of the receptors occurs,[17,18]

Multipling through by (K_d+free) produces,

$$\text{Bound}\ (K_d + \text{free}) = \frac{B_{max} \times \text{free}}{K_d + \text{free}}\ (K_d + \text{free}) \qquad \text{(Eq. A2)}$$

$$K_d \times \text{Bound} + \text{free} \times \text{Bound} = B_{max} \times \text{free} \qquad \text{(Eq. A3)}$$

Rearrange,

$$K_d \times \text{Bound} = B_{max} \times \text{free} - \text{free} \times \text{Bound} = \text{free}\ (B_{max} - \text{Bound}) \qquad \text{(Eq. A4)}$$

Divide through,

$$\frac{\text{Bound}}{\text{free}} = \frac{B_{max} - \text{Bound}}{K_d} = \frac{B_{max}}{K_d}\left(1 - \frac{\text{Bound}}{B_{max}}\right) \qquad \text{(Eq. A5)}$$

A dose of 5 mCi (185 MBq) ^{123}I-IBZM at no-carrier added level $\equiv$20 pmol IBZM

If the brain uptake is 5% of the dose, 1 pmol$\pm$ IBZM is in the brain. B_{max} is ~15 pmol/m*l*. Because the total volume of basal ganglia is assumed to be 20 m*l*, the total D_2 receptor number in the brain is 300 pmol.[6]

$\therefore$ The entire dose on receptors would occupy 1/300 or $\ll$1% of the receptors, which is negligible and not significantly affected by the dose. Even if we take into account the presence of residual BZM with its 50-fold lower affinity, receptor occupancy is only 3%.

From (Eq. A5), Bound/B_{max} is fraction saturated.

$\therefore$ at low saturation,

$$\frac{\text{Bound}}{\text{free}} = \frac{B_{max}}{K_d} \qquad \text{(Eq. A6)}$$

The activity of basal ganglia (BG) means the (Bound+free), and the uptake of frontal cortex (FC) means the free radioligand.

$$\therefore \quad \frac{BG}{FC} = \frac{\text{Bound} + \text{free}}{\text{free}} = \frac{\text{Bound}}{\text{free}} + 1 = \frac{B_{max}}{K_d} + 1 \qquad \text{(Eq. A7)}$$

Rearrange

$$\frac{B_{max}}{K_d} = \frac{BG}{FC} - 1$$

$$B_{max} = \left(\frac{BG}{FC} - 1\right) \times K_d \qquad \text{(Eq. A8)}$$

ACKNOWLEDGMENTS

The authors gratefully acknowledge Dr. Hank F. Kung, Department of Radiology, University of Pennsylvania for valuable cooperation in providing us with the precursor BZM, Nordion International Inc., Vancouver for providing us with part of the sodium ^{123}I-iodide, and Douglas C. Vines, B.A.Sc., R.T.N.M. for technical support.

REFERENCES

1. Verhoeff NPLG: Pharmacological implications for neuroreceptor imaging. *Eur J Nucl Med* 18: 482–502, 1991
2. Baron JC, Mazière B, Loc'h C, et al: Loss of striatal [^{76}Br] bromospiperone binding sites demonstrated by positron tomography in progressive supranuclear palsy. *J Cereb Blood Flow Metab* 11: 220–228, 1991
3. Budinger TF: Advances in emission tomography: Quo vadis? [Editorial] *J Nucl Med* 31: 628–631, 1990
4. Kung HF, Pan S, Kung MP, et al: *In vitro* and *in vivo*

evaluation of [^{123}I]IBZM: A potential CNS D-2 dopamine receptor imaging agent. *J Nucl Med* 30: 88–92, 1989
5. Brücke T, Tsai YF, Mclellan C, et al: *In vitro* binding properties and autoradiographic imaging of 3-iodobenzamide ([^{125}I]-IBZM): A potential imaging ligand for D-2 dopamine receptors in SPECT. *Life Sci* 42: 2097–2104, 1988
6. Kung HF, Alavi A, Chang W, et al: *In vivo* SPECT imaging of CNS D-2 dopamine receptors: Initial studies with iodine-123-IBZM in humans. *J Nucl Med* 31: 573–579, 1990
7. Costa DC, Verhoeff NPLG, Cullum ID, et al: *In vivo* characterization of 3-iodo-6-methoxybenzamide ^{123}I in humans. *Eur J Nucl Med* 16: 813–816, 1990
8. Brücke T, Podreka I, Angelberger P, et al: Dopamine D2 receptor imaging with SPECT: Studies in different neuropsychiatric disorders. *J Cereb Blood Flow Metab* 11: 220–228, 1991
9. Verhoeff NPLG, Brücke T, Podreka I, et al: Dynamic SPECT in two healthy volunteers to determine the optimal time for *in vivo* D2 dopamine receptor imaging with ^{123}I-IBZM using the rotating gamma camera. *Nucl Med Commun* 12: 687–697, 1991
10. Mazière B, Loc'h C, Raynaud C, et al: I-123 Iodolisuride, a new SPECT imaging ligand for brain dopamine D2 receptors [Abstract]. *J Nucl Med* 30: 731–732, 1989
11. Yonekura Y, Iwasaki Y, Saji H, et al: SPECT imaging of dopamine D-2 receptor: Kinetics of I-123 2′-iodospiperone in normal subjects [Abstract]. *J Nucl Med* 31: 885, 1990
12. Kung MP, Kung HF, Billings J, et al: The characterization of IBF as a new selective dopamine D-2 receptor imaging agent. *J Nucl Med* 31: 648–654, 1990
13. Ichise M, Toyama H, Fornazzari L, et al: Assessment of subjects with and at risk for developing Huntington's disease by I-123 IBZM and Tc-99m HM-PAO SPECT [Abstract]. *J Nucl Med* 33: 970, 1992
14. Tatsch K, Schwarz J, Oertel WH, et al: SPECT imaging of dopamine D2 receptors with ^{123}I-IBZM: Initial experience in controls and patients with Parkinson's syndrome and Wilson's disease. *Nucl Med Commun* 12: 699–707, 1991
15. Kung MP, Liu BL, Yang YY, et al: A kit formulation for preparation of iodine-123-IBZM: A new CNS D-2 dopamine receptor imaging agent. *J Nucl Med* 32: 339–342, 1991
16. Farde L, Hall H, Ehrin E, et al: Quantitative analysis of D2 dopamine receptor binding in living human brain by PET. *Science* 231: 258–261, 1986
17. Farde L, Eriksson L, Blomquist G, et al: Kinetic analysis of central [^{11}C]raclopride binding to D_2-dopamine receptors studied by PET—A comparison to the equation analysis. *J Cereb Blood Flow Metab* 9: 696–708, 1989
18. Sedvall G, Farde L, Persson A, et al: Imaging of neurotransmitter receptors in the living human brain. *Arch Gen Psychiatry* 43: 995–1005, 1986
19. Kebabian JW, Calne DB: Multiple receptors for dopamine. *Nature* 277: 93–96, 1979
20. Bunzow JR, Van Tol HHM, Grandy DK, et al: Cloning and expression of a rat D_2 dopamine receptor cDNA [Letter]. *Nature* 336: 783–787, 1988
21. Giros B, Sokoloff P, Martes MP, et al: Alternative splicing directs the expression of two D_2 dopamine receptor isoforms [Letter]. *Nature* 342: 923–926, 1989
22. Monsma FJ, McVittie LD, Gerfen CR, et al: Multiple D_2 dopamine receptors produced by alternative RNA splicing [Letter]. *Nature* 342: 926–929, 1989
23. Dal Toso R, Sommer B, Ewert M, et al: The dopamine D_2 receptor: two molecular forms generated by alternative splicing. *EMBO J* 8: 4025–4034, 1989
24. Sokoloff P, Giros B, Martres MP, et al: Molecular cloning and characterization of a novel dopamine receptor (D_3) as a target for neuroleptics. *Nature* 347: 146–151, 1990
25. Van Tol HHM, Bunzow JR, Guan HC, et al: Cloning of the gene for a human dopamine D_4 receptor with high affinity for the antipsychotic clozapine [Letter]. *Nature* 350: 610–614, 1991
26. Sunahara RK, Guan HC, O'Dowd BF, et al: Cloning of the gene for a human dopamine D_5 receptor with higher affinity for dopamine than D_1 [Letter]. *Nature* 350: 614–619, 1991
27. Beaulieu M: Clinical importance of D-1 and D-2 receptors. *Can J Neurol Sci* 14: 402–406, 1987
28. Wagner HN, Burns HD, Dannals RF, et al: Imaging dopamine receptors in the human brain by positron tomography. *Science* 221: 1264–1266, 1983
29. Crawley JCW, Smith T, Veall N, et al: Dopamine receptors displayed in living human brain with ^{77}Br-p-bromospiperone. *Lancet* 2: 975, 1983
30. Seeman P, Niznik HB, Guan HC: Elevation of Dopamine D_2 receptors in schizophrenia is underestimated by radioactive raclopride [Letter]. *Arch Gen Psychiatry* 47: 1170–1172, 1990
31. Misra CH, Shelat HS, Smith RC: Effect of age on adrenergic and dopaminergic receptor binding in rat brain. *Life Sci* 27: 521–526, 1980
32. Marquis JK, Lippa AS, Pelham RW: Dopamine receptor alterations with aging in mouse and rat corpus striatum. *Biochem Pharmacol* 30: 1876–1878, 1981
33. Severson JA, Marcusson J, Winbland B, et al: Age-correlated loss of dopaminergic binding sites in human basal ganglia. *J Neurochem* 39: 1623–1631, 1982
34. Morgan DG, Marcusson JA, Nyberg P, et al: Divergent changes in D-1 and D-2 dopamine binding sites in human brain during aging. *Neurobiol Aging* 8: 195–201, 1987
35. Guttman M, Seeman P: Dopamine D2 receptor density in Parkinsonian brain is constant for duration of disease, age, and duration of L-dopa therapy. *Adv Neurol* 45: 51–57, 1986
36. Brooks DJ, Ibanez V, Sawle GV, et al: Striatal D_2 receptor status in patients with Parkinson's disease, Striatonigral degeneration, and Progressive supranuclear palsy, measured with ^{11}C-raclopride and positron emission tomography. *Ann Neurol* 31: 184–192, 1992

37. Seeman P, Guan HC, Niznik HB: Endogenous dopamine lowers the dopamine D_2 receptor density as measured by [^{3}H]raclopride: Implications for positron emission tomography of the human brain. *Synapse* 3: 96–97, 1989
38. Young LT, Wong DF, Goldman S, et al: Effects of endogenous dopamine on kinetics of [^{3}H]N-methylspiperone and [^{3}H]raclopride binding in the rat brain. *Synapse* 9: 188–194, 1991
39. Innis RB, Malison RT, Tikriti MAL, et al: Amphetamine-stimulated dopamine release competes *in vivo* for [^{123}I]IBZM binding to the D_2 receptor in non-human primates. *Synapse* 10: 177–184, 1992
40. Wong DF, Wagner HN, Dannals RF, et al: Effects of age on dopamine and serotonin receptors measured by positron tomography in the living human brain. *Science* 226: 1393–1396, 1984
41. Iyo M, Yamasaki T, Fukuda H, et al: Age-related decrease of ^{11}C-N-methylspiperone *in vivo* binding to human striatum detected by PET. *Kaku Igaku* 26: 213–220, 1989
42. Thal LJ, Horowitz SG, Dvorkin B, et al: Evidence for loss of brain [^{3}H]spiroperidol and [^{3}H]ADTN binding sites in rabbit brain with aging. *Brain Res* 192: 185–194, 1980
43. Leenders KL, Frackowiak RSJ, Quinn N, et al: Brain energy metabolism and dopaminergic function in Huntington's disease measured *in vivo* using positron emission tomography. *Movement disorders* 1: 69–77, 1986